Pharm Res (2012) 29:3302–3311
DOI 10.1007/s11095-012-0822-5

RESEARCH PAPER

Prediction of the Vitreal Half-Life of Small Molecular Drug-Like Compounds

Heidi Kidron • Eva M. del Amo • Kati-Sisko Vellonen • Arto Urtti

Received: 6 May 2012 / Accepted: 22 June 2012 / Published online: 10 July 2012

ABSTRACT

Purpose To build a fast, user-friendly computational model to predict the intravitreal half-lives of drug-like compounds.

Methods We used multivariate analysis to build intravitreal half-life models using two data sets, one with experimental data derived from both pigmented and albino rabbits and another including only data from experiments with albino rabbits.

Results The final models had a Q^2 value of 0.65 and 0.75 for the mixed and albino rabbit models, respectively. The models performed well in predicting the intravitreal half-life of an external test set. In addition, the models are physiologically interpretable, containing mainly hydrogen bonding and lipophilicity descriptors.

Conclusion The developed models enable reliable predictions of intravitreal half-lives for use in the early drug development stages, without the need for prior experimental data.

KEY WORDS blood-retinal barrier · intravitreal injection · multivariate analysis · ocular drug delivery · QSPR

H. Kidron (✉) • E. M. del Amo • A. Urtti
Centre for Drug Research, Faculty of Pharmacy, University of Helsinki
P.O. Box 56, FIN-00014 Helsinki, Finland
e-mail: heidi.kidron@helsinki.fi

E. M. del Amo • K.-S. Vellonen
Division of Biopharmacy and Pharmacokinetics, Faculty of Pharmacy
University of Helsinki
Helsinki, Finland

Present Address:
K.-S. Vellonen
School of Pharmacy, University of Eastern Finland
Kuopio, Finland

ABBREVIATIONS

FRB	freely rotatable bonds
HA	number of hydrogen bond acceptors
HD	number of hydrogen bond donors
H_{tot}	total number of putative hydrogen bonds, i.e. HD +HA
logP	the logarithm of the octanol-water partition coefficient of the neutral form
log $t_{½}$	the logarithm of the intravitreal half-life, $logD_x$, the logarithm of the octanol-water partition coefficient at pH x
MW	molecular weight
PCA	principal component analysis
P-gp	P-glycoprotein
PLS	partial least squares
QSPR	quantitative structure-property relationship
RMSE	root mean squared error
RMSEP	root mean squared error of prediction
VIP	variable importance in the projection

INTRODUCTION

Intravitreal therapy is used to treat ocular diseases in the posterior segments of the eye, for example, age-related macular degeneration and diabetic macular edema. Intravitreal drug administration must be used, because topical eye drop treatment does not lead to adequate drug concentrations in the posterior target sites (retina, choroid, vitreous). The drug is injected directly into the vitreous, which is a hydrophilic gel consisting of a network of well separated hyaluronic acid and collagen type II fibers, allowing diffusion of drug molecules, even macromolecules, to the retina and choroid. One advantage of the intravitreal injections is

that it generally leads to minimal systemic exposure of the drug. However, due to the invasive nature of the injections, other ways of delivering drugs to the posterior eye segment have been attempted, but the topical, systemic and subconjunctival delivery routes generally fail in reaching effective concentrations in the vitreous body (1).

After an injection into the vitreous there are two routes by which the molecule can be eliminated: 1) anteriorly via flows of aqueous humor and uveal blood circulation; 2) posteriorly through the blood-retinal barrier to retinal and choroidal blood circulation (2). The blood-retinal barrier is composed of the retinal pigment epithelium and the tight walls of retinal capillary. The cells in the blood-retinal barrier express transporters, which in principle may affect drug elimination from the vitreous, but the effect of transporters on drug elimination *in vivo* is still unclear (3). The posterior route presents a large surface area surrounding the vitreous, but the cells in the blood-retinal barrier form a tight layer, allowing efficient elimination of lipophilic compounds. The anterior route, in contrast, is limited by the small area that is available for diffusion from the vitreous into the posterior and anterior chambers. In general, elimination through the posterior route takes place rapidly, whereas drug elimination via the anterior route is slower (2).

Intravitreal drugs can be administered as injections or implants that release drug over prolonged times. In all cases, drug concentrations in vitreous are dependent on the rate of drug elimination from the vitreous. Slow intravitreal drug elimination is desirable, since it will prolong the duration of drug action after intravitreal injections and minimizes the required drug loading in the controlled release formulations. The intravitreal half-life of a compound must be determined *in vivo* by injecting the compound into the vitreous of an animal, usually rabbit, and measuring the concentration of the compound in the vitreous at certain time-points after the injection. Pharmacokinetic evaluation is typically carried out using many time points (often 5–10) and several replicates of each time point is needed (more than 5). Thus, for plotting a reliable time-concentration curve at least 20 animals are needed, which makes this method unacceptable for drug screening. There is a need for an alternative method that would enable screening of molecules before *in vivo* studies and also reduce and refine animal experiments related to development of ocular drugs and intravitreal drug delivery systems.

A computational method like quantitative structure-property relationships (QSPR) modeling is optimal for rapid virtual evaluation and pre-selection of compounds. Even though QSPR models are widely used to study the relationship between physicochemical properties and the pharmacokinetic properties of molecules, surprisingly few attempts have been made to predict the intravitreal half-life of injected drugs. Some prior studies have established that compounds with a high molecular weight are preferably eliminated by the anterior route (4), and that molecular weight (MW) and lipophilicity do have an influence on the intravitreal half-life (5–7). However, some studies (5,6) have been done using small sets of structurally and chemically similar compounds and, therefore, those models are not broadly applicable to diverse compounds. Durairaj and co-workers used a large set of molecules, including small molecules and macromolecules, with a MW range from 32 to 149 000 Da, but explored only a limited set of variables, including only molecular weight, lipophilicity and solubility variables to derive QSPR models by multiple regression (7).

We aimed to build a computational model for virtual prediction of drug elimination from the vitreous. The models are focused on compounds with molecular weight below 1500 Da, thus excluding macromolecules. The use of a lower, narrower MW range will make the model more applicable for prediction of small molecules. We have made a careful literature search and collected experimental data on the intravitreal half-lives of 47 compounds in albino and pigmented rabbits. The data set contains molecules with diverse structural and chemical features. The relationship between the intravitreal half-life and 33 physicochemical descriptors was determined by multivariate analysis. Simple mathematical equations were derived, enabling reliable prediction of the intravitreal half-life for a compound without any experimental data.

MATERIALS AND METHODS

Compound Data Set

A data set of 47 compounds (Table I) was collected from an an extensive literature search for intravitreal injections (5,8–49). The half-lives of the compounds included in the dataset have been measured in either albino or pigmented rabbits. A subset was constructed from this dataset, containing 39 compounds with experimental data collected from only albino rabbits (Table I). An average value was calculated for compounds with more than one reference. The model is focused on molecules with molecular weight less than 1500 Da. In addition, we only included data from experiments with compounds that were dissolved in water or buffer solution and injected into normal, healthy eyes. When the intravitreal half-life had not been reported for a compound, the half-life was calculated from the reported concentrations. Compounds for which the intravitreal concentrations had been measured during a time-span that was less than two half-lives, were excluded from the data set.

Data that was deemed of insufficient quality due to for instance large standard deviations or an irregular time-concentration curve was also excluded. For two-compartment models, the half-life of the terminal phase was used, except for moxifloxacin and fluorouracil, where the alpha phase was dominant.

Table I Calculated Descriptors Used in the Final Models and Experimentally Determined Intravitreal Half-Life of Compounds in the Data Sets

compound	albino/pigmented	$t_{1/2}$ (h)mix	$t_{1/2}$ (h)alb	H_{tot}	$LogD_{7.4}$	FRB	Reference
1-heptanol	albino	2.6	2.6	2	2.37	6	(8)
1-pentanol[b,d]	albino	1.2	1.2	2	1.35	4	(8)
1-propanol	albino	1.0	1.0	2	033	2	(8)
Å6 peptide	albino	19.4	19.4	38	−8.68	28	(9)
acyclovir[d]	albino	3.0	3.0	12	−0.62	5	(10)
amikacin[a,c]	albino	25.9	25.9	35	−10.59	22	(11)
ampicillin[b]	albino	8.8	8.8	11	−1.84	5	(12)
aztreonam	albino/pigmented	7.9	8.3	18	−4.32	7	(12,13)
candesartan	abino	6.8	6.8	11	1.45	7	(14)
carbenicillin	albino/pigmented	4.3	3.5	11	−3.62	5	(15,16)
cefazolin	albino	3.8	3.8	14	−4.41	7	(17)
cefepime[a]	pigmented	14.6	–	15	−2.29	7	(18,19)
ceftazidime[b]	pigmented	18.0	–	18	−2.95	9	(19)
ceftizoxime	pigmented	5.7	–	14	−4.35	5	(19)
ceftriaxone[c]	albino/pigmented	11.6	14.1	20	−4.58	8	(19,20)
cephalexin[d]	albino	3.1	3.1	11	−2.93	5	(17)
cephalothin	albino	2.4	2.4	10	−3.62	7	(17)
cidofovir[a]	albino	21.0	21.0	14	−5.41	7	(21)
ciprofloxacin	albino	4.4	4.4	8	−0.29	3	(5)
clarithromycin[b,d]	albino	2.0	2.0	18	2.06	12	(22)
clindamycin[c]	albino	3.0	3.0	11	0.70	10	(23)
cyclosporin A	albino	7.6	7.6	28	2.79	16	(24)
dexamethasone[b]	pigmented	3.5	–	8	2.03	5	(25)
fleroxacin[a]	albino	3.4	3.4	7	−3.09	4	(5)
fluconazole[d]	albino	3.2	3.2	8	0.45	6	(26)
fluorescein	albino	2.5	2.5	7	2.68	2	(27,28)
fluorouracil	pigmented	12.8	–	6	−1.64	0	(29)
ganciclovir[b]	albino/pigmented	6.0	5.3	14	−0.74	7	(10,30–32)
gentamicin[c]	albino/pigmented	22.7	22.0	23	−7.81	13	(33,34)
grepafloxacin[a]	albino/pigmented	3.5	3.5	8	0.62	3	(35)
kanamycin[b,d]	albino	10.3	10.3	30	−8.86	17	(36)
lincomycin	albino	12.6	12.6	13	−0.36	11	(37)
methanol	albino	0.9	0.9	2	−0.69	0	(8)
methicillin	albino	6.2	6.2	10	−2.71	5	(38)
methotrexate[c]	albino	7.6	7.6	20	−5.10	9	(39)
moxalactam[a]	albino	16.1	16.1	19	−7.31	10	(40)
moxifloxacin	pigmented	1.7	–	9	0.31	4	(41)
netilmicin[b,d]	albino	26.6	26.6	23	−6.79	14	(12,42)
ofloxacin[b]	albino	3.0	3.0	8	−0.39	2	(5)
penicillin	not known	4.2	–	8	−1.81	4	(43,44)
piperacillin	albino	8.9	8.9	15	−2.73	6	(12)
quinidine[a]	albino	2.0	2.0	5	0.98	5	(28,45)
sparfloxacin[c]	albino	2.8	2.8	11	0.83	4	(5)
tobramycin	albino	31.5	31.5	29	−9.54	16	(46)
trifluorothymidine[b]	albino	3.2	3.2	10	−0.20	4	(47)

Table I (continued)

compound	albino/pigmented	$t_{1/2}$ (h)mix	$t_{1/2}$ (h)alb	H_{tot}	$LogD_{7.4}$	FRB	Reference
vancomycin	pigmented	62.3	–	54	−4.49	23	(48)
voriconazole[d]	albino	2.5	2.5	7	1.21	6	(49)

[a] The compound was excluded from the mixed data set prior to model building and included in the external test set, [b] The compound was selected to the internal test set from the mixed data set based on the PCA, [c] The compound was excluded from the albino data set prior to model building and included in the external test set, [d] The compound was selected to the internal test set from the albino data set based on the PCA.

Molecular Descriptors

The chemical structure of the compounds in the data set were retrieved from ACD/Dictionary (50), or the the PubChem database (http://pubchem.ncbi.nlm.nih.gov/). The ACDLabs software package version 12 was used to calculate the molecular descriptors for these compounds (50). A total of 33 descriptors were chosen for this study; pKa, LogD at pH 2, 5.5, 6.5, 7, 7.4 and 10, LogP, MW, PSA (polar surface area), FRB (freely rotatable bonds), HD (hydrogen bond donors), HA (hydrogen bond acceptors), H_{tot} (HD+HA), molar refractivity, molar volume, parachor, index of refraction, surface tension, density, polarizability, C ratio, N ratio, NO ratio, hetero ratio, halogen ratio, number of rings and number of aromatic, 3-, 4-, 5- and 6-membered rings.

Multivariate Data Analysis

Before data analysis, an external data set of seven compounds was randomly extracted from the collected data set of 47 compounds from pigmented and albino rabbits (mixed set), while six compounds were randomly extracted from the albino data set of 39 compounds (Table I). The compounds in the external data sets were not used for model building or training. A logarithmic transformation was performed for those variables that had a broad range or were not equally distributed over the range. A principal component analysis (PCA) including all molecular descriptors was calculated to analyze the diversity of the data set. The logarithm of intravitreal half-life ($log_{t1/2}$) was correlated to the molecular descriptors by Partial Least Squares (PLS) analysis using Simca-P (version 10.5) (51). Based on the distribution of the compounds in the PCA plot training sets of 30 and 25 compounds and internal test sets of ten compounds and eight compounds were generated, respectively, for the mixed and albino data set. Only the compounds in the training set were used to calculate the models. Both cross-validation and prediction of the intravitreal half-life of the compounds in the internal tests sets were used to evaluate the predictive capability of the models. For cross-validation, the training set is divided into seven groups and the intravitreal half-life for the compounds in each group is predicted using the data in the other groups. The sum of squared errors between the actual and predicted data is calculated and converted into the Q^2 value (cross validated R^2). The half-life for the compounds in the internal test sets were predicted for further evaluation of the models. Ultimately, the final models were assessed by predicting the half-life of the external data sets that were extracted before data analysis (Table I).

The statistical significance of the models was assessed by Y-scrambling, i.e. the model is fitted to scrambled half-life values and R^2Y (equivalent to the R^2 coefficient) and Q^2 are calculated. After repeating the process 50 times, the results are plotted with the R^2Y values on the Y-axis and the Q^2 values on the X-axis and regression lines are fitted to the points. For statistically valid models, the intercepts should be below 0.3 and 0.05 for R^2Y and Q^2, respectively.

RESULTS

Literature Search

Initially, we found 83 reported intravitreal half-lives for compounds by literature searches. Twenty of these half-lives were excluded from the data set, since they did not fulfill the criteria as described in the Materials and Methods section. Among the compounds that were left out from the data set is triamcinolone acetonide, which is a well-studied and widely used drug in ocular therapy. However, it was excluded from the study as it is poorly soluble and precipitates in the vitreous after injection, thus, its long half-life is due to the slow dissolution of the drug particles in the vitreous. The remaining 63 reported half-lives were used to build the mixed data set of 47 compounds, containing data from both pigmented and albino rabbits, as well as the subset of 39 compounds from albino rabbits (Table I). An average value was calculated for those compounds with more than one study that reported a half-life. The terminal half-life, in the case of two-compartment models, was used as the elimination half-life in all cases except two: moxifloxacin and fluorouracil. For moxifloxacin the half-life of the first phase was used, since it is the dominant phase, while an effective half-life was calculated for fluorouracil, taking into account both the first phase (alpha) and the terminal phase (beta), ($t_{1/2,\ eff}$=(AUC_{alpha}/AUC_{tot})x $t_{1/2alpha}$+(AUC_{beta}/AUC_{tot})x $t_{1/2beta}$)(52). For fluorouracil, the first phase accounted for approximately one third of the total

elimination based on the AUC of the alpha phase. Therefore, the effective half-life deviates from terminal half-life and is a more representative indicator for drug concentration decay in the vitreous. The unusual elimination profile of moxifloxacin might be due to its ability to strongly bind to melanin (53).

Molecular Diversity of the Compounds

The compounds in the mixed data set cover a broad range of structurally and chemically diverse molecules, with an intravitreal half-life from 0.9 to 62.3 h. The molecular weights of the compounds varied from 32 to 1449 Da and the $LogD_{7.4}$ from -10.60 to 2.68. All calculated descriptors were used to perform PCA for both mixed and albino dataset (Fig. 1). The mixed data set resulted in a PCA model with five principal components that explained 81% of the variance in the data set, while the PCA model for the albino data set contained four principal components explaining 80% of the variance. The PCA score plots of the two first principal components, explaining 44% and 18%, respectively, of the variance in the mixed data set and 42% and 18%, respectively, of the variance in the albino data set, are shown in Fig. 1. Methanol lies outside the elliptic 95% tolerance volume of both the mixed and albino PCA models, but it was not excluded from model building, since 5% of the data set is allowed outside the tolerance volume. The compounds in the data sets were divided into training sets (30 and 25 compounds in the mixed and albino training sets, respectively) and internal test sets (10 and 8 compounds in the mixed and albino test sets, respectively) based on their distribution in the PCA score plot (Fig. 1, Table I).

PLS Analysis of Training Set Compounds and Evaluation of Derived Models with Internal Test Set Compounds

The PLS model using all the 33 calculated descriptors and the 30 compounds of the mixed training set had a R^2Y= 0.65 and Q^2=0.59, and the PLS model with all descriptors

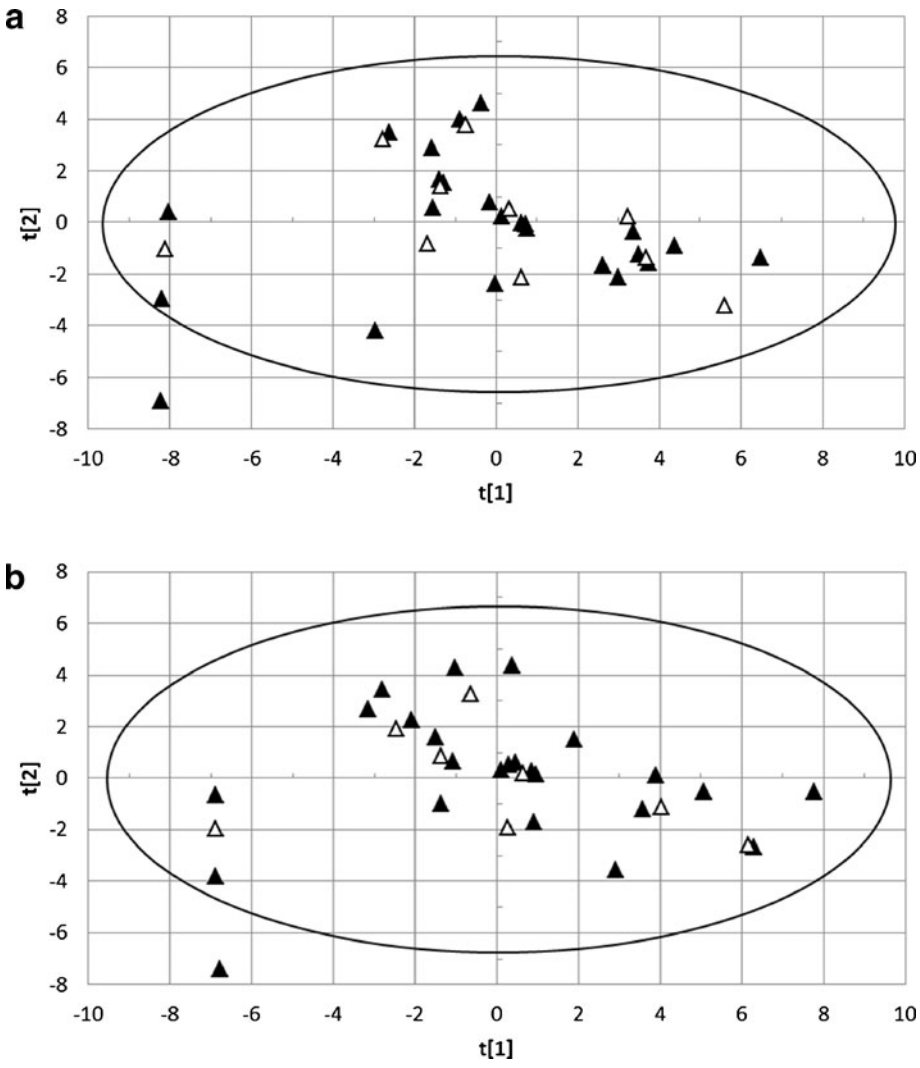

Fig. 1 PCA score plot of (**a**) the 47 compounds in the mixed data set and (**b**) the 39 compounds in the albino data set. The black triangles represent compounds in the training set and the unfilled triangles the compounds in the internal test set. The ellipse depicts the 95% tolerance volume based on hotelling T^2 (0.05).

for the albino set had similar values, R^2Y=0.69 and Q^2= 0.55 (Table II). In order to construct a simpler model, we excluded those descriptors that according to SIMCAs variable influence on projection (VIP) function were deemed the least influential (Fig. 2). A VIP value above 1 specifies the descriptor as more influential than average in explaining the modeled response. A threshold of 1.2 and 1.1 was chosen for the mixed and the albino data set, respectively, leading to models with 14 descriptors for both data sets. The models had improved statistics with higher R^2 and Q^2 values than the initial models (Table II). The descriptors were related to lipophilicity (LogD at pH 5.5, 6.5, 7 and 7.4), hydrogen bonding (H_{tot}, HD, HA and PSA) and mass (MW, MV, polarizability, molar refractivity and parachor), as well as the amount of rotatable bonds, defined with the variable FRB. Subsequently, we excluded the descriptors with high correlation coefficients (> 0.9) with H_{tot}, $LogD_{7.4}$ or MW. The H_{tot} variable was chosen since it combined the information from the HD and HA descriptors, which it is highly correlated to. The MW descriptor was selected since it had the highest VIP value of the correlated coefficients, while the $LogD_{7.4}$ descriptor was chosen for its physiological relevance. This resulted in a four-variable model for both data sets, including the descriptors H_{tot}, MW, $LogD_{7.4}$ and FRB. Both models had good statistics, with R^2Y=0.64, Q^2=0.61 for the mixed model and R^2Y=0.73, Q^2=0.71 in the albino model. The predictability of these models was evaluated on the internal test set, with a Q^2int value of 0.61 and 0.67 for the mixed and albino model, respectively. Exclusion of the FRB descriptor in the mixed model improved the statistics and the prediction of the internal test set (Table II), while creating a three-variable model by removing any of the other descriptors led to markedly decreased predictability of the internal test set (data not shown). Similarly, exclusion of the MW descriptor in the albino data set improved the model statistics and predictability of the internal test set, while creating a three-variable model by exclusion of any of the other variables did not have a beneficial impact. Furthermore, a two-variable model with good statistics and better predictability for the internal data set was obtained for the mixed data sets using only the H_{tot} and $LogD_{7.4}$ descriptors (Table II). A two-variable model for the albino data using the same descriptors resulted in a model with a lower Q^2 value, but good predictability of the internal test set.

The two-variable model was chosen for the mixed data set, while the three-variable model was chosen for the albino data set for further evaluation. The final models are described by the following equations:

$$\log t_{1/2,\text{mixed}} = -0.046 - 0.051(\log D_{7.4}) + 0.640(\text{Log}H_{tot})$$

$$\log t_{1/2,\text{albino}} = -0.164 - 0.032(\log D_{7.4}) + 0.435(\text{Log}H_{tot}) + 0.461(\text{Log}(\text{FRB} + 1))$$

The statistical significance of the predictive capability of these final models was evaluated with the *validate* function in Simca-P. The R^2Y and Q^2 Y-intercepts were -0.06 and -0.16 for the mixed model and -0.02 and -0.18 for the albino model, respectively. Both are well below the upper limits of a statistically valid model.

Evaluation of the Final Models on an External Test Set

The final models were used to predict the intravitreal half-life of the compounds in the external data sets that were removed prior to model building (Table I). Both models predicted the compounds in the external data sets with good accuracy, with an external Q^2 value of 0.81 and 0.88, respectively, for the mixed and albino models.

Table II PLS Models Obtained from the Mixed Data Set Compounds and the Albino Dataset Compounds

Variables	A[a]	R^2X	Training set		RMSEE[b]	Internal test set	
			R^2Y	Q^2		Q^2	RMSEP[c]
Mixed data set							
33	1	0.42	0.65	0.59	0.256	0.68	0.229
14	1	0.72	0.66	0.63	0.252	0.60	0.255
Htot, MW, $LogD_{7.4}$, FRB	1	0.74	0.64	0.61	0.260	0.61	0.255
Htot, MW, $LogD_{7.4}$	1	0.75	0.66	0.65	0.232	0.63	0.245
Htot, $LogD_{7.4}$	1	0.80	0.66	0.64	0.250	0.69	0.225
Albino data set							
33	1	0.43	0.69	0.55	0.220	0.70	0.256
14	1	0.68	0.72	0.68	0.206	0.74	0.263
Htot, MW, $LogD_{7.4}$, FRB	1	0.74	0.73	0.71	0.205	0.67	0.287
Htot, $LogD_{7.4}$, FRB	1	0.75	0.75	0.75	0.196	0.74	0.276
Htot, $LogD_{7.4}$	1	0.79	0.70	0.66	0.218	0.76	0.239

[a]Number of principal components in the PLS model. [b]RMSEE, Root Mean Squared Error of Estimation. [c]RMSEP, Root Mean Squared Error of Prediction

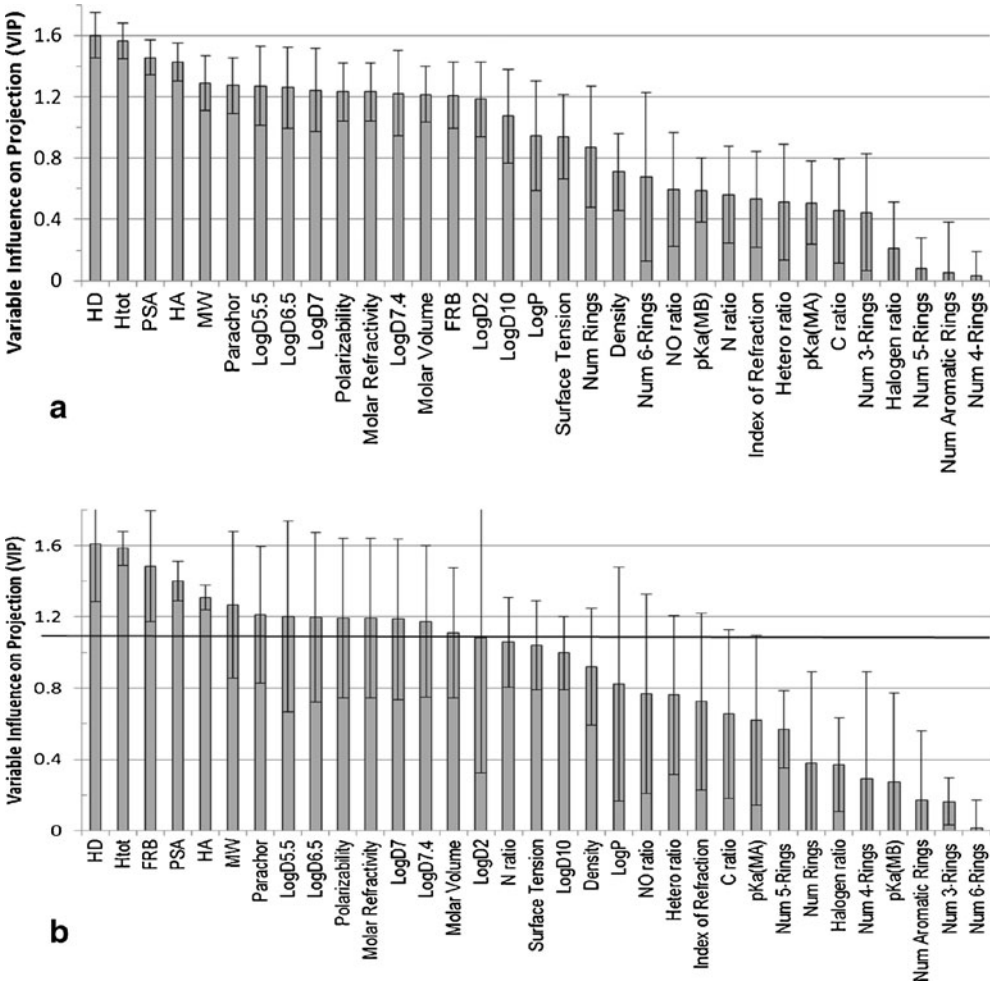

Fig. 2 VIP plots, with confidence intervals, from PLS analysis using all variables and the training set compounds for (**a**) the mixed data set and (**b**) the albino data set. A horizontal line has been drawn in (**b**) to indicate the 1.1 VIP threshold.

DISCUSSION

Two models for the prediction of intravitreal half-life were obtained, one specifically for albino rabbits and one that is suitable both for albino and pigmented rabbits. Due to the limited amount of data available for pigmented rabbits (only 13 compounds), we did not attempt to build a specific model for pigmented rabbits. Both of the final models had good statistical values, with the R^2Y and Q^2 of the albino higher (both values 0.75) compared to those of the mixed set model (0.66 and 0.64, respectively). The ability of the models to predict the intravitreal half-life was verified both on internal test sets as well as on randomly selected external test sets (Fig. 3). The models performed well, as the difference in observed and predicted half-life for the most poorly predicted compound in the mixed test sets was 2.3-fold (cidofovir in the external test set) and all in all, only four other compounds had more than a two-fold difference to the experimental value. In the albino test sets, clarithromycin was predicted to have a 3.4-fold longer half-life than observed experimentally, but on the other hand, there was only one other compound, kanamycin, with a two-fold error in its predicted half-life, while all the other compounds had less than two-fold error-prediction.

The final models contained only two or three variables, H_{tot} and $LogD_{7.4}$ in the model for the mixed data set, and H_{tot}, $LogD_{7.4}$ and FRB for the albino set. Both models had better R^2Y and Q^2 values than the models using all 33 calculated variables and also slightly improved values compared to the four-variable models (Table II). Furthermore, the variables that are included in the final models are easily interpretable. A higher $LogD_{7.4}$ value leads to a shorter half-life, which is likely due to increased permeability of the cell membranes in the blood-retinal barrier, while increasing the amount of hydrogen bond donors and acceptors results in longer half-lives, as polar compounds have more difficulties to permeate membranes. According to the albino model, flexible compounds that have a high amount of rotatable bonds have longer half-lives.

Previous studies have linked intravitreal half-life to MW and lipophilicity (4–7). In our study, MW was also an influential descriptor with a relatively high VIP value, but still its exclusion improved the predictivity of the models. One possible explanation is that our model focuses on low MW

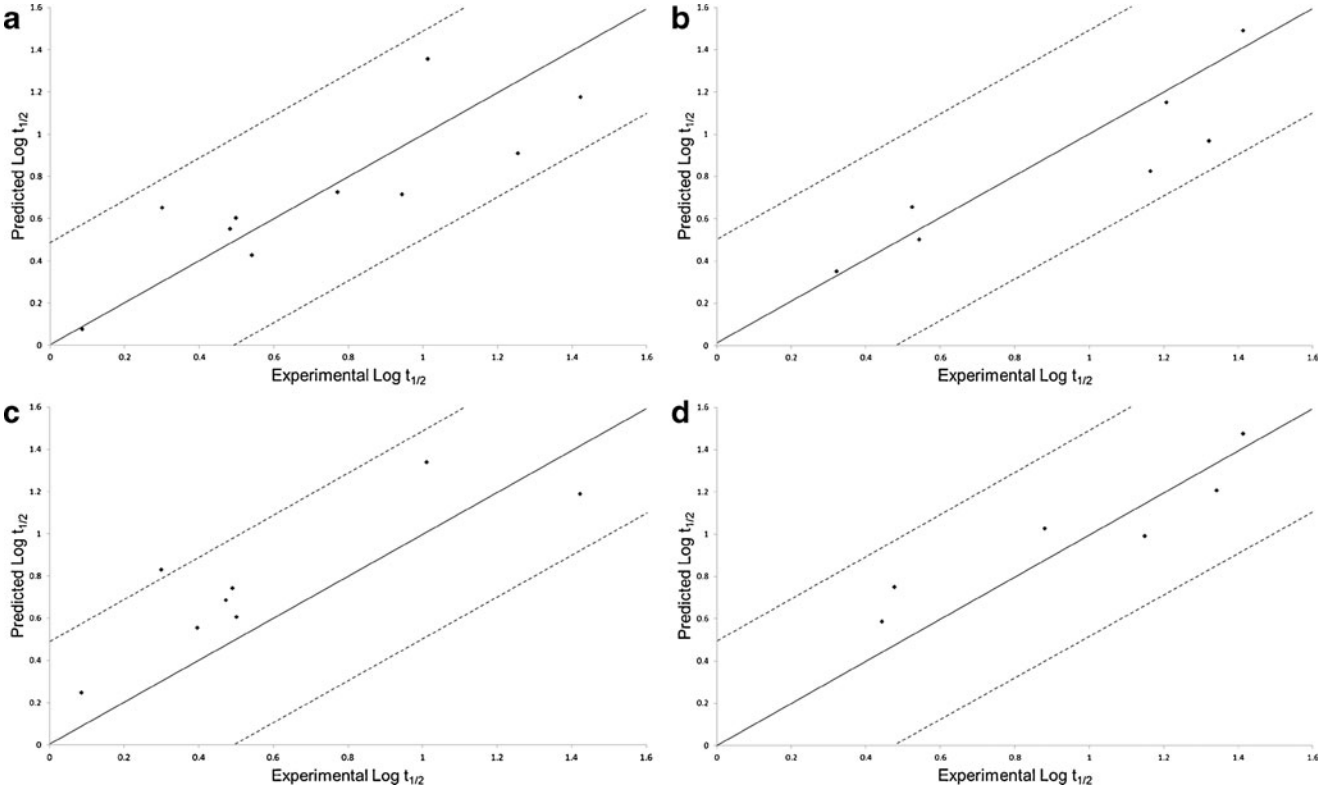

Fig. 3 Predicted *versus* observed log $t_{1/2}$ values based on the final models. Prediction of the mixed data set compounds in the internal test set (**a**) and external test set (**b**) and the albino data set compounds in the internal test set (**c**) and external test set (**d**). A diagonal line has been drawn in $R^2Y = 1$ to facilitate interpretation and the dashed lines represent a 3-fold prediction range.

compounds and, thus, does not highlight the effect MW on the half-life, and a more clear effect might only be observed when significantly larger compounds, like macromolecules with MW of several thousand Da are included. Macromolecules, like proteins, have a slower rate of diffusion in the vitreous and they are predominantly eliminated from the vitreous through the anterior route. These compounds have significantly longer half-lives than molecules that can permeate the blood-retinal barrier. However, we have only included compounds that have MW <1500 Da in our study, and therefore this size effect may not be evident in our data set. Another likely explanation could be that the number of rotatable bonds as well as hydrogen bonds generally tends to increase with the size of molecules and, therefore, the successful use of MW in describing membrane permeability is due to its correlation with increased polarity and flexibility (54), which in our model is described by the H_{tot} and FRB variables. However, Veber and co-workers found that the number of FRB influences membrane permeability of compounds independently of MW (54).

Some compounds in the data set are known substrates for transporters in the retinal pigment epithelium cells. For example, carbenicillin and quinidine have been identified as substrates for P-glycoprotein (P-gp) (15,28,45). Interestingly, these compounds are not outliers in our model, which might be due to the relatively small increase (1.5–2.5-fold) in intravitreal half-life of these compounds when a P-gp inhibitor is coadministered. For the same reason the model is quite accurate in predicting the half-lives of these transporter substrates, as the effect of active transport apparently falls within the 3-fold prediction error of the model for the compounds in this study. The lack of influence of active transport on the estimation of half-lives suggests that active transport is not highly significant for intravitreal elimination for the compounds included in this study.

The two models that were generated in this study are quite similar, which either can point to similar pharmacokinetics in

Table III Comparison of Half-Lives Obtained in Both Albino and Pigmented Rabbits

compound	$t_{1/2}$,albino (h)	$t_{1/2}$, pigmented (h)	references
aztreonam	8.3	7.5	(12,13)
carbenicillin	3.5	5	(15,16)
ceftriaxone	14.1	9.1	(19,20)
ganciclovir	5.24*	7.9	(10,30–32)
gentamicin	22*	24	(33,34)
grepafloxacin	3.5	3.5	(35)

*average value

the eye of albino and pigmented rabbits, or to a bias of albino rabbits due to the majority of data acquired from albino rabbits. However, based on a comparison of the half-lives of six compounds for which the half-life had been reported both in albino and pigmented rabbits (Table III), there is no clear trend for longer elimination times in either albino or pigmented, suggesting similar rate of vitreal elimination. It is well known that many drugs are able to bind to the pigmentation (e.g. ganciclovir (10,30–32), gentamicin (33,34) and grepafloxacin (35) in our data set) and this may affect drug distribution in the tissues, such as retinal pigment epithelium. This is not reflected in the elimination rate constants, because even though some fraction of the intravitreally injected drug would bind to the melanin granules in the retinal pigment epithelium, it will mostly enter plasma that acts as a sink rather than distributing back to the vitreous.

The QSPR model presented is expected to be a useful tool in ocular drug research. The model will provide an early virtual estimate of the drug elimination rate. Thus, it will be easy to estimate drug concentration profiles after intravitreal injections at different dosing levels. With straightforward modeling approaches concentration predictions can be extended to administration of suspensions and drug delivery systems. In that case, drug dissolution or release rate can be used as input rate and the QSPR based elimination as output rate. There are some limitations in the use of the QSPR model. Firstly, we recommend that the models are used to predict the intravitreal half-life for compounds in the same chemical space as the test compounds, i.e. the descriptor values should be in the same range as the descriptor values in the model. Secondly, the half-lives in the human eye may not be the same as in the rabbit eye. The dimensions of the human eye are slightly bigger than in the rabbit eye, but the physiological factors of drug elimination (blood retina barrier, aqueous humor flow, blood aqueous humor barrier) are similar. Geometrical scaling methods can be used to obtain estimates for elimination in human eyes.

CONCLUSIONS

We have built a QSPR model for the prediction of intravitreal half-life of drug-like compounds. The model encompasses a broad chemical space and 33 *in silico* descriptors were used to build an optimal model. Overall, the QSPR model will be a useful tool in ocular drug discovery and development as it will help to reduce and refine animal experiments.

ACKNOWLEDGMENTS AND DISCLOSURES

The Academy of Finland, Magnus Ehrnooth Foundation, Medicinska Understödsföreningen för Liv och Hälsa, Orion-Farmos Research Foundation, and the Graduate School in Pharmaceutical Research are acknowledged for their support.

REFERENCES

1. Del Amo EM, Urtti A. Current and future ophthalmic drug delivery systems. A shift to the posterior segment. Drug Discov Today. 2008;13(3–4):135–43.
2. Maurice DM, Mishima S. Ocular pharmacokinetics. In: Sears ML, editor. Handbook of experimental pharmacology. Berlin-Heidelberg: Springer Verlag; 1984. p. 16–119.
3. Mannermaa E, Vellonen KS, Urtti A. Drug transport in corneal epithelium and blood-retina barrier: emerging role of transporters in ocular pharmacokinetics. Adv Drug Deliv Rev. 2006;58 (11):1136–63.
4. Maurice DM. Injection of drugs into the vitrous body. In: Leopold IH, Burns RP, editors. Symposium on ocular therapy. New York: Wiley; 1976. p. 59–72.
5. Liu W, Liu QF, Perkins R, Drusano G, Louie A, Madu A, *et al.* Pharmacokinetics of sparfloxacin in the serum and vitreous humor of rabbits: physicochemical properties that regulate penetration of quinolone antimicrobials. Antimicrob Agents Chemother. 1998;42 (6):1417–23.
6. Dias CS, Mitra AK. Vitreal elimination kinetics of large molecular weight FITC-labeled dextrans in albino rabbits using a novel microsampling technique. J Pharm Sci. 2000;89(5):572–8.
7. Durairaj C, Shah JC, Senapati S, Kompella UB. Prediction of vitreal half-life based on drug physicochemical properties: quantitative structure-pharmacokinetic relationships (QSPKR). Pharm Res. 2009;26(5):1236–60.
8. Atluri H, Mitra AK. Disposition of short-chain aliphatic alcohols in rabbit vitreous by ocular microdialysis. Exp Eye Res. 2003;76 (3):315–20.
9. Koh HJ, Cheng L, Bessho K, Jones TR, Davidson MC, Freeman WR. Intraocular properties of urokinase-derived antiangiogenic A6 peptide in rabbits. J Ocul Pharmacol Ther. 2004;20(5):439–49.
10. Hughes P, Krishnamoorthy R, Mitra A. Vitreous disposition of two acylguanosine antivirals in the albino and pigmented rabbit models: a novel ocular microdialysis technique. J Ocular Pharmacol Ther. 1996;12:209–24.
11. Zheng S, Hu C, Wei H, Lu Y, Zhang Y, Yang J, *et al.* Intravitreal pharmacokinetics of liposome-encapsulated amikacin in a rabbit model. Ophtalmology. 1993;100(11):1640–4.
12. Miglioli PA, Dorigo MT. Antibiotic levels in aqueous and vitreous humor after intraocular administration. Chemotherapy. 1989;35 (6):406–9.
13. Barza M, McCue M. Pharmacokinetics of aztreonam in rabbit eyes. Antimicrob Agents Chemother. 1983;24(4):468–73.
14. Lee JE, Lim DW, Park HJ, Shin JH, Lee SM, Oum BS. Intraocular toxicity and pharmacokinetics of candesartan in a rabbit model. Invest Ophthalmol Vis Sci. 2011;52(6):2924–9.
15. Schenk AG, Peyman GA, Paque JT. The intravitreal use of carbenicillin (Geopen) for treatment of pseudomonas endophalmitis. Acta Ophthalmol (Copenh). 1974;52:707–17.
16. Barza M, Kane A, Baum J. The effects of infection and probenecid on the transport of carbenicillin from the rabbit vitreous humor. Invest Ophthalmol Vis Sci. 1982;22(6):720–6.
17. Macha S, Mitra AK. Ocular pharmacokinetics of cephalosporins using microdialysis. J Ocul Pharmacol Ther. 2001;17(5):485–98.
18. Jay WM, Shockley RK. Toxicity and pharmacokinetics of cefepime (BMY-28142) following intravitreal injection in pigmented rabbit eyes. J Ocul Pharmacol 1988 Winter;4(4):345-349.

19. Barza M, Lynch E, Baum JL. Pharmacokinetics of newer cephalosporins after subconjunctival and intravitreal injection in rabbits. Arch Ophthalmol. 1993;111(1):121–5.
20. Shockley RK, Jay WM, Friberg TR, Aziz AM, Rissing JP, Aziz MZ. Intravitreal ceftriaxone in a rabbit model. Dose- and time-dependent toxic effects and pharmacokinetic analysis Arch Ophthalmol. 1984;102(8):1236–8.
21. Dolnak DR, Munguia D, Wiley CA, De Clercq E, Bergeron-Lynn GL, Boscher C, *et al.* Lack of retinal toxicity of the anticytomegalovirus drug (S)-1-(3-hydroxy-2-phosphonylmethoxypropyl) cytosine. Invest Ophthalmol Vis Sci. 1992;33(5):1557–63.
22. Unal M, Peyman GA, Liang C, Hegazy H, Molinari LC, Chen J, *et al.* Ocular toxicity of intravitreal clarithromycin. Retina. 1999;19(5):442–6.
23. Fiscella R, Peyman GA, Fishman PH. Duration of therapeutic levels of intravitreally injected liposome-encapsulated clindamycin in the rabbit. Can J Ophthalmol. 1987;22(6):307–9.
24. Pearson PA, Jaffe GJ, Martin DF, Cordahi GJ, Grossniklaus H, Schmeisser ET, *et al.* Evaluation of a delivery system providing long-term release of cyclosporine. Arch Ophthalmol. 1996;114(3):311–7.
25. Kwak HW, D'Amico DJ. Evaluation of the retinal toxicity and pharmacokinetics of dexamethasone after intravitreal injection. Arch Ophthalmol. 1992;110(2):259–66.
26. Gupta SK, Velpandian T, Dhingra N, Jaiswal J. Intravitreal pharmacokinetics of plain and liposome-entrapped fluconazole in rabbit eyes. J Ocul Pharmacol Ther. 2000;16(6):511–8.
27. Anand BS, Atluri H, Mitra AK. Validation of an ocular microdialysis technique in rabbits with permanently implanted vitreous probes: systemic and intravitreal pharmacokinetics of fluorescein. Int J Pharm. 2004 Aug 20;281(1–2):79–88.
28. Majumdar S, Hippalgaonkar K, Srirangam R. Vitreal kinetics of quinidine in rabbits in the presence of topically coadministered P-glycoprotein substrates/modulators. Drug Metab Dispos. 2009 Aug;37(8):1718–25.
29. Jarus G, Blumenkranz M, Hernandez E, Sossi N. Clearance of intravitreal fluorouracil. Normal and aphakic vitrectomized eyes Ophthalmology. 1985 Jan;92(1):91–6.
30. Macha S, Mitra AK. Ocular disposition of ganciclovir and its monoester prodrugs following intravitreal administration using microdialysis. Drug Metab Dispos. 2002 Jun;30(6):670–5.
31. Lopez-Cortes LF, Pastor-Ramos MT, Ruiz-Valderas R, Cordero E, Uceda-Montanes A, Claro-Cala CM, *et al.* Intravitreal pharmacokinetics and retinal concentrations of ganciclovir and foscarnet after intravitreal administration in rabbits. Invest Ophthalmol Vis Sci. 2001 Apr;42(5):1024–8.
32. Macha S, Duvvuri S, Mitra AK. Ocular disposition of novel lipophilic diester prodrugs of ganciclovir following intravitreal administration using microdialysis. Curr Eye Res. 2004 Feb;28 (2):77–84.
33. Peyman GA, May DR, Ericson ES, Apple D. Intraocular injection of gentamicin. Toxic effects of clearance Arch Ophthalmol. 1974 Jul;92(1):42–7.
34. Kane A, Barza M, Baum J. Intravitreal injection of gentamicin in rabbits. Effect of inflammation and pigmentation on half-life and ocular distribution Invest Ophthalmol Vis Sci. 1981 May;20 (5):593–7.
35. Solans C, Bregante MA, Garcia MA, Perez S. Ocular penetration of grepafloxacin after intravitreal administration in albino and pigmented rabbits. Chemotherapy. 2004 Jun;50(3):133–7.
36. Peyman GA, Nelsen P, Bennett TO. Intravitreal injection of kanamycin in experimentally induced endophthalmitis. Can J Ophthalmol. 1974 Jul;9(3):322–7.
37. Schenk AG, Peyman GA. Lincomycin by direct intravitreal injection in the treatment of experimental bacterial endophthalmitis. Albrecht Von Graefes Arch Klin Exp Ophthalmol. 1974;190 (4):281–91.
38. Daily MJ, Peyman GA, Fishman G. Intravitreal injection of methicillin for treatment of endophthalmitis. Am J Ophthalmol. 1973 Sep;76(3):343–50.
39. Velez G, Yuan P, Sung C, Tansey G, Reed GF, Chan CC, *et al.* Pharmacokinetics and toxicity of intravitreal chemotherapy for primary intraocular lymphoma. Arch Ophthalmol. 2001 Oct;119 (10):1518–24.
40. Leeds NH, Peyman GA, House B. Moxalactam (Moxam) in the treatment of experimental staphylococcal endophthalmitis. Ophthalmic Surg. 1982 Aug;13(8):653–6.
41. Iyer MN, He F, Wensel TG, Mieler WF, Benz MS, Holz ER. Clearance of intravitreal moxifloxacin. Invest Ophthalmol Vis Sci. 2006 Jan;47(1):317–9.
42. Sloane H, Peyman GA, Raichand M, West S. Netilmicin: new aminoglycoside effective against bacterial endophthalmitis. Can J Ophthalmol. 1981 Jan;16(1):22–6.
43. Gardiner PA, Michaelson IC, Rees RJ, Robson JM. The Effects of various Types of Penicillin Injected into the Vitreous. Br J Ophthalmol. 1948 Oct;32(10):768–75.
44. Duguid JP, Ginsberg M, Fraser IC, Macaskill J, Michaelson IC, Robson JM. Experimental Observations on the Intravitreous use of Penicillin and Other Drugs. Br J Ophthalmol. 1947 Apr;31 (4):193–211.
45. Duvvuri S, Gandhi MD, Mitra AK. Effect of P-glycoprotein on the ocular disposition of a model substrate, quinidine. Curr Eye Res. 2003 Dec;27(6):345–53.
46. Kim EK, Kim HB. Pharmacokinetics of intravitreally injected liposome-encapsulated tobramycin in normal rabbits. Yonsei Med J. 1990 Dec;31(4):308–14.
47. Pang MP, Branchflower RV, Chang AT, Peyman GA, Blatt H, Minatoya HK. Half-life and vitreous clearance of trifluorothymidine after intravitreal injection in the rabbit eye. Can J Ophthalmol. 1992 Feb;27(1):6–9.
48. Coco RM, Lopez MI, Pastor JC, Nozal MJ. Pharmacokinetics of intravitreal vancomycin in normal and infected rabbit eyes. J Ocul Pharmacol Ther. 1998 Dec;14(6):555–63.
49. Shen YC, Wang MY, Wang CY, Tsai TC, Tsai HY, Lee YF, *et al.* Clearance of intravitreal voriconazole. Invest Ophthalmol Vis Sci. 2007 May;48(5):2238–41.
50. Advanced Chemistry Developement, Toronto, Canada.
51. Umetrics AB, Box 7960, SE-90719 Umeå, Sweden. Simca-P. ;10.5.
52. Boxenbaum H, Battle M. Effective half-life in clinical pharmacology. J Clin Pharmacol. 1995 Aug;35(8):763–6.
53. Siefert HM, Kohlsdorfer C, Steinke W, Witt A. Pharmacokinetics of the 8-methoxyquinolone, moxifloxacin: tissue distribution in male rats. J Antimicrob Chemoter 1999 May; 43 SupplB: 61-67
54. Veber DF, Johnson SR, Cheng HY, Smith BR, Ward KW, Kopple KD. Molecular properties that influence the oral bioavailability of drug candidates. J Med Chem. 2002 Jun 6;45(12):2615–23.